Optimization of the buffer dielectric layer for the creation of low-defect epitaxial films of the topological insulator $Pb_{1-x}Sn_xTe$ with $x \geq 0.4$

© A.K. Kaveev[1], O.E. Tereshchenko[2]

[1] Ioffe Institute,
194021 St. Petersburg, Russia
[2] Rzhanov Institute of Semiconductor Physics, Siberian Branch, Russian Academy of Sciences,
630090 Novosibirsk, Russia
E-mail: kaveev@mail.ioffe.ru

Received March 2, 2022
Revised March 25, 2022
Accepted March 25, 2022

We have optimized the growth conditions of the buffer layer for further deposition of $Pb_{1-x}Sn_xTe$ ($x \geq 0.4$), which has the properties of a crystalline topological insulator. To this end, a three-component heterostructure consisting of CaF_2, BaF_2, and $Pb_{0.7}Sn_{0.3}Te$: In layers was formed and optimized on the Si(111) surface. The surface morphology of this structure was studied depending on the temperature growth regimes and the optimal combination of growth parameters was selected from the point of view of smoothness and crystalline quality.

Keywords: crystalline topological insulator, molecular beam epitaxy, reflection high-energy electron doffraction, atomic force microscopy, $Pb_{0.7}Sn_{0.3}Te$: In.

DOI: 10.21883/SC.2022.07.54760.08

1. Introduction

Crystalline topological insulators (TIs) based on the $Pb_{1-x}Sn_xTe$ compound are promising from the point of view of practical applications [1], due to the possibility of creating TIs with a volume more weakly shunting the conductivity of topological states on account of the possibility for controlling the composition (value x), in contrast to the already become classical TIs based on V_2VI_3 compounds. In addition to composition control, it is equally important to obtain low-defect $Pb_{1-x}Sn_xTe$ films, also from the point of view of reducing the shunting effect of the volume. This problem is nontrivial due to the problems arising during the epitaxial growth of $Pb_{1-x}Sn_xTe$, such as insufficient layer smoothness and insufficient crystalline quality. To ensure the presence of conducting topological states, it is necessary to obtain the planar layer with high crystalline quality.

It is known that for the epitaxial growth of $Pb_{1-x}Sn_xTe$ films on silicon, binary buffer BaF_2/CaF_2/Si(111) layers [2] were used. Together with, the height of the surface relief of the obtained buffer layers was too high due to the insufficient optimization of the growth parameters and the defectiveness of these layers. In this work, optimization of the buffer layer for further deposition of $Pb_{1-x}Sn_xTe$ ($x \geq 0.4$), which has topological properties, has been carried out. To do this, the multilayer structure consisting of layers CaF_2, BaF_2 and $Pb_{0.7}Sn_{0.3}Te$: In was deposited to the surface of Si(111). It is known [3] that calcium fluoride, when deposited to the (111) silicon surface by molecular beam epitaxy, forms layers of high crystalline quality, but with different surface morphology, in relation to the deposition temperature. The formation of islands of various heights and lateral sizes is possible. The aim of the present work was to provide as smoothest surface as possible.

The films were grown by molecular-beam epitaxy in the set providing ultra high vacuum up to 10^{-8} Pa. The set was equipped with the RHEED gun, quartz microbalance, and the block of effusion cells. In the work, each of the grown materials was evaporated from its own effusion cell.

2. Results and discussion

To ensure the smoothness of the surface of buffer layer, the temperature conditions and the thickness of calcium fluoride layer were varied. Next, the layer of barium fluoride was deposited on the surface of calcium fluoride, providing a smoother transition in the lattice constant from CaF_2 to $Pb_{1-x}Sn_xTe$.

Fig. 1, *a–g* shows a number of atomic force microscopy patterns of the BaF_2/CaF_2/Si(111) heterostructure of various configurations. A number of parameters were determined that provide a combination of small thicknesses of fluorite sublayers (which ensures their low imperfection) with their high smoothness. It has been shown that a decrease in the growth temperature of calcium fluoride and barium fluoride leads to decrease in the lateral dimensions of the islands. The smoothest surface relief is achieved at low growth temperatures (250°C). This correlates with the results of the paper [4], where the high planarity of calcium fluoride films with thickness of one nanometer deposited at given temperature was demonstrated.

Attempts to increase the growth temperature of one of the two sublayers in order to improve the crystalline quality lead to an enlargement of the islands and coarsening of the relief, which is undesirable for the task of obtaining

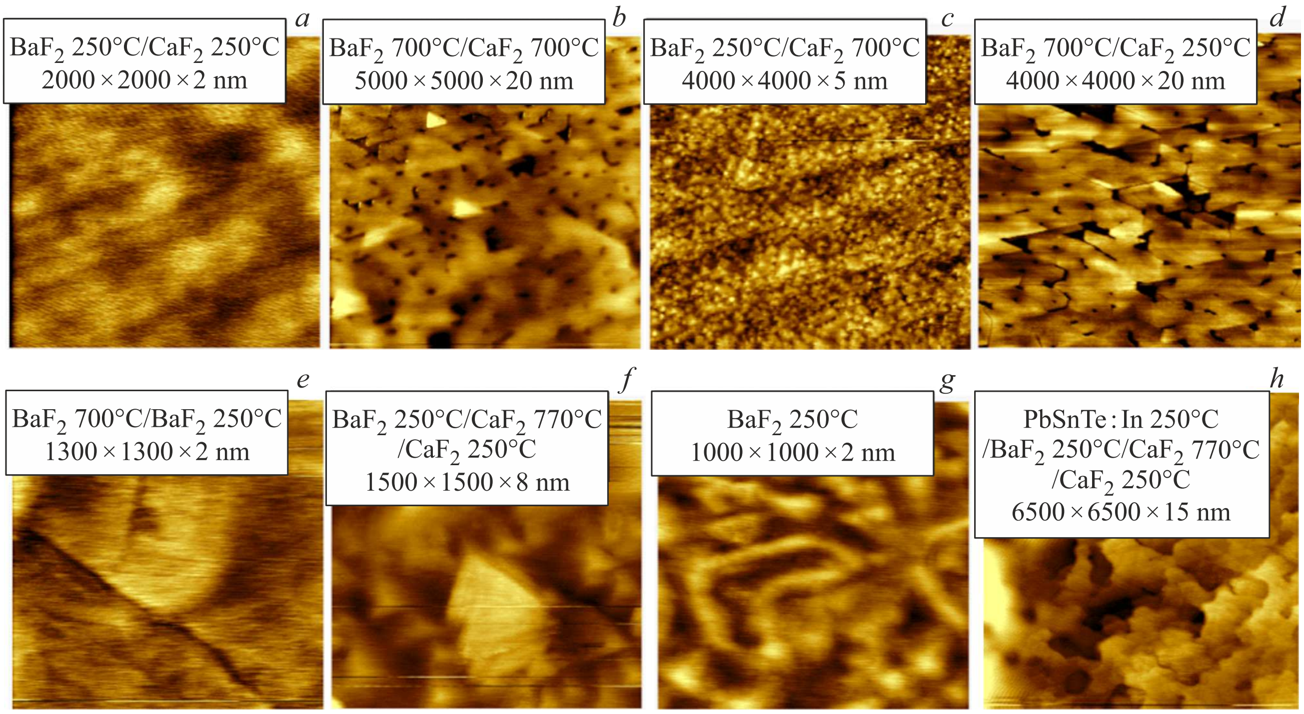

Figure 1. Surface morphology of the buffer layer BaF_2/CaF_2 (*a*–*g*), grown under various conditions, and $Pb_{0.7}Sn_{0.3}Te$: In/BaF_2/CaF_2/Si(111) heterostructure with optimized layered buffer (*h*). *a*–*d* — the thickness of BaF_2 and CaF_2 20 and 10 nm, respectively. Layer thicknesses: *e* — 10 and 3 nm, *f* — 15, 7 and 3 nm, *g* — 20 nm , *h* — 300, 15, 7 and 3 nm.

the maximal smooth layers set in this work. It is also sometimes possible to form cracks in the film due to the difference in thermal expansion coefficients. At the same time, sufficiently smooth relief is also obtained by using two-stage (low and high temperatures) calcium fluoride growth, followed by low-temperature deposition of a barium fluoride layer (Fig. 1,*f*).

Together with, direct deposition of the thin layer of $Pb_{1-x}Sn_xTe$ on the double-layered buffer does not provide sufficient smoothness and sufficient crystalline quality for the formation of topological states. Good quality can be achieved only with the help of homoepitaxial growth of this material on sufficiently thick sublayer. Moreover, it is also necessary to achieve a low conductivity of this sublayer by doping it, which ensures the regulation for the position of the Fermi level.

The experiments performed with fluorite double-layered buffer made it possible to proceed to experiments with the deposition of the third buffer sublayer — dielectric $Pb_{0.7}Sn_{0.3}Te$: In. This sublayer was grown at various temperatures: from 250 to 450°C (Fig. 1,*h* and 2). The experiments performed also showed the importance for deposition of large (> 500 nm) thicknesses of this sublayer to ensure its continuity, the absence of holes in the film, and to achieve high surface planarity.

Fig. 2 shows examples of the surface morphology of the third buffer sublayer obtained under different conditions. The dielectric properties of this sublayer will be measured at the next stage of work by electrophysical measurements. In the future, thin (10–20 nm) layers of stoichiometry close to $Pb_{0.6}Sn_{0.4}Te$ with excess of Sn will be deposited on this sublayer, providing the presence of conducting topological states.

The evolution of the surface during the formation of a three-layered buffer was studied *in situ* using reflection high-energy electron diffraction (RHEED). Fig. 3 shows the change in RHEED patterns upon successive deposition of 10 nm calcium fluoride (*a*), 15 nm barium fluoride (*b*) and 1000 nm $Pb_{0.7}Sn_{0.3}Te$: In at the initial (*c*) and final moment (*d*) of growth at temperature of 250°C. It can be seen that calcium and barium fluorides grow in planar manner, as evidenced by the strands in the RHEED patterns. Further, at the initial stage of growth, the three-dimensional (island) growth of $Pb_{0.7}Sn_{0.3}Te$: In occurs. Twinning of the reflections indicates a two-domain growth mode, which is specific for a cubic crystal lattice with (111) growth plane. In our earlier paper [5], trial experiments on deposition of thin $Pb_{0.7}Sn_{0.3}Te$ films on Si(111) using a calcium fluoride buffer sublayer, were carried out. The following epitaxial relations were established regarding silicon: (111)$Pb_{0.7}Sn_{0.3}Te$ ‖ (111) Si, $[1\bar{2}1]$ $Pb_{0.7}Sn_{0.3}Te$ ‖ [211]Si. In the present case, these relations are obviously retained.

With an increase of the thickness of the deposited material, spot-like reflections are replaced by streaks, which indicates the overgrowth of islands (the Stranski–Krastanov

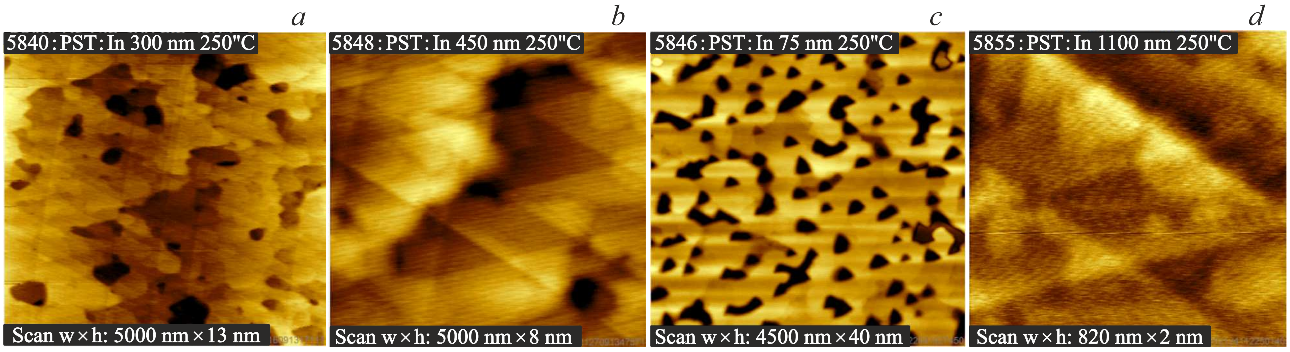

Figure 2. Surface morphology of the third buffer $Pb_{0.7}Sn_{0.3}Te$: In in relation to the growth conditions. *a* — deposition of $Pb_{0.7}Sn_{0.3}Te$: In on BaF_2/CaF_2 bilayer with parameters corresponding to Fig. 1, *f*; *b* — the same, but thinner layer $Pb_{0.7}Sn_{0.3}Te$: In; *c* — deposition of $Pb_{0.7}Sn_{0.3}Te$: In on BaF_2/CaF_2 bilayer with parameters, corresponding to Fig. 1, *a*; *d* — the same, but thinner layer of $Pb_{0.7}Sn_{0.3}Te$: In, and at a lower temperature.

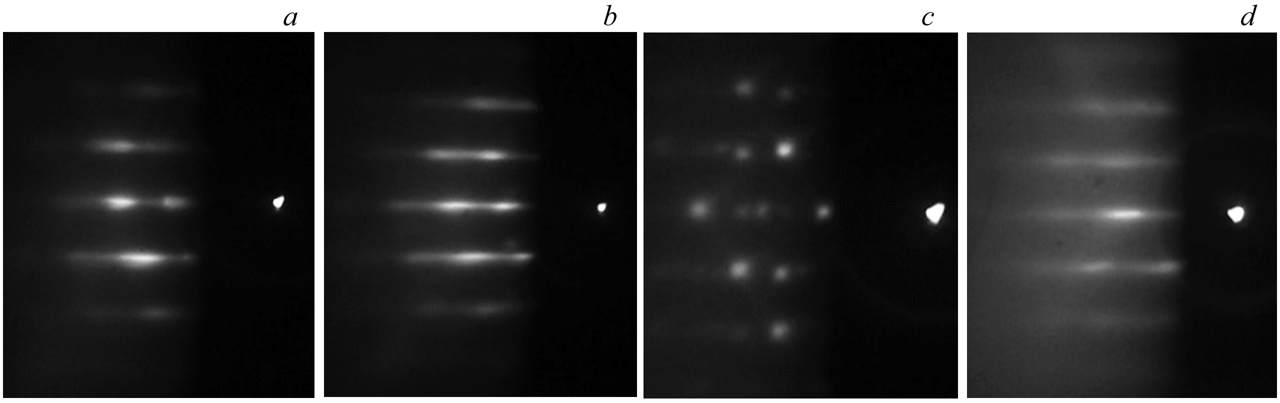

Figure 3. Change in RHEED patterns upon deposition of 10 nm calcium fluoride (*a*), 15 nm barium fluoride (*b*) and 1000 nm $Pb_{0.7}Sn_{0.3}Te$: In at the initial moment (*c*) and at the final moment (*d*) of growth at temperature of 250°C.

growth mode) and the formation of a smooth surface. This RHEED pattern (Fig. 3, *d*) is in accordance to Fig. 2, *d*, where a smooth surface with characteristic lines at an angle of 60° is indeed demonstrated. The lines are the dislocation outcrops, that are also characteristic of the growth surface (111) of the cubic crystal lattice.

3. Conclusion

As a result, in this work, for multi-layered epitaxial structure $Pb_{0.7}Sn_{0.3}Te$: In/BaF_2/CaF_2/Si(111) a number of growth modes are considered and growth parameters are optimized. The possibility of planar low-defect growth of the third sublayer: $Pb_{0.7}Sn_{0.3}Te$: In, necessary for further homoepitaxial growth of $Pb_{1-x}Sn_xTe$ with increased value of the parameter $x \geq 0.4$ in order to obtain surface topological states, is shown.

Funding

The study was supported by the Russian Foundation for Basic Research grant No. 21-52-12024 NNIO_a.

Conflict of interest

The authors declare that they have no conflict of interest.

References

[1] T.H. Hsieh, H. Lin, J. Liu, W. Duan, A. Bansil, L. Fu. Nature Commun., **3**, 982 (2012).
[2] A.N. Akimov, A.V. Belenchuk, A.E. Klimov, M.M. Kachanova, I.G. Neizvestny, S.P. Suprun, O.M. Shapoval, V.N. Sherstyakova, V.N. Shumsky. Techn. Phys. Lett., **35**, 524 (2009).
[3] C.A. Lucas, D. Loretto, G.C.L. Wong. Phys. Rev. B, **50**, 14340 (1994).
[4] Y.Y. Illarionov, A.G. Banshchikov, D.K. Polyushkin, S. Wachter, T. Knobloch, M. Thesberg, L. Mennel, M. Paur, M. Stoger-Pollach, A. Steiger-Thirsfeld, M.I. Vexler, M. Waltl, N.S. Sokolov, T. Mueller, T. Grasser. Nature Electronics, **2**, 230 (2019).
[5] A.K. Kaveev, D.N. Bondarenko, O.E. Tereshchenko. FTP, **55** (8), 625 (2021) (in Russian).